

Altered brain morphology and functional connectivity in postmenopausal women: automatic segmentation of whole-brain and thalamic subnuclei and resting-state fMRI

Gwang-Won Kim¹, Kwangsung Park^{1,2}, Yun-Hyeon Kim³, Gwang-Woo Jeong³

¹Advanced Institute of Aging Science, Chonnam National University, Gwangju 61186, Republic of Korea

²Department of Urology, Chonnam National University Hospital, Chonnam National University Medical School, Gwangju 61469, Republic of Korea

³Department of Radiology, Chonnam National University Hospital, Chonnam National University Medical School, Gwangju 61469, Republic of Korea

Correspondence to: Gwang-Woo Jeong; email: gwieong@jnu.ac.kr

Keywords: brain morphology, functional connectivity, sex hormones, thalamic subnuclei

Received: August 22, 2023

Accepted: February 7, 2024

Published: March 23, 2024

Copyright: © 2024 Kim et al. This is an open access article distributed under the terms of the [Creative Commons Attribution License](https://creativecommons.org/licenses/by/4.0/) (CC BY 4.0), which permits unrestricted use, distribution, and reproduction in any medium, provided the original author and source are credited.

ABSTRACT

The transition to menopause is associated with various physiological changes, including alterations in brain structure and function. However, menopause-related structural and functional changes are poorly understood. The purpose of this study was not only to compare the brain volume changes between premenopausal and postmenopausal women, but also to evaluate the functional connectivity between the targeted brain regions associated with structural atrophy in postmenopausal women. Each 21 premenopausal and postmenopausal women underwent magnetic resonance imaging (MRI). T1-weighted MRI and resting-state functional MRI data were used to compare the brain volume and seed-based functional connectivity, respectively. In statistical analysis, multivariate analysis of variance, with age and whole brain volume as covariates, was used to evaluate surface areas and subcortical volumes between the two groups. Postmenopausal women showed significantly smaller cortical surface, especially in the left medial orbitofrontal cortex (mOFC), right superior temporal cortex, and right lateral orbitofrontal cortex, compared to premenopausal women ($p < 0.05$, Bonferroni-corrected) as well as significantly decreased functional connectivity between the left mOFC and the right thalamus was observed ($p < 0.005$, Monte-Carlo corrected). Although postmenopausal women did not show volume atrophy in the right thalamus, the volume of the right pulvinar anterior, which is one of the distinguished thalamic subnuclei, was significantly decreased ($p < 0.05$, Bonferroni-corrected). Taken together, our findings suggest that diminished brain volume and functional connectivity may be linked to menopause-related symptoms caused by the lower sex hormone levels.

INTRODUCTION

Aging is a multifaceted and complex phenomenon characterized by physiological changes that exert a variety of effects on the structure and function of the brain [1]. One such pivotal transition in women is menopause, which encompasses the loss of ovarian reproductive function [2–4]. This transition, indicative of aging, leads to a decline in female sex hormones,

such as estrogen. This decline has been linked to an elevated risk of neurodegenerative diseases, notably Alzheimer's disease (AD) [5–7].

Estrogen plays a pivotal role in modulating neurotransmitter systems, neurotrophins, and brain cytoarchitecture [8–15]. These interactions might affect estrogen's influence on neural systems governing mood and cognition. Notably, postmenopausal women have a

higher risk of AD than men, and this sex difference risk has been hypothesized to be associated with the loss of estrogens following menopause [16]. The biological mechanisms underlying the increased AD risk in women are not fully understood [17]. Therefore, further studies are needed to evaluate the neurophysiological changes in postmenopausal women.

The investigation of menopause-related brain structural and functional alterations in women provides a unique opportunity to evaluate the early detection of neurodegenerative disease. Several studies [1, 6, 16, 18–20] have indicated a potential connection between menopause and brain volume, possibly mediated by the decrease in female sex hormones following menopause. For example, one structural magnetic resonance imaging (MRI) study [1] reported that postmenopausal women showed decreased gray matter volumes in the supplementary motor area, inferior frontal gyrus, olfactory cortex, and superior temporal gyrus compared to premenopausal women, which suggests that reduced volumes were closely associated with menopause-related symptoms. A similar study [20] demonstrated accelerated reduction of the hippocampal volume in postmenopausal women. Several morphometric studies [6, 16, 18, 19] focusing on the effects of estrogen therapy (ET) in postmenopausal women demonstrated enhanced cognitive function that are possibly associated with improvement of the corresponding brain structure and/or connectivity.

Consistent with the structural imaging findings, functional neuroimaging studies [21–23] reported that functional abnormalities in postmenopausal women were associated with cognitive impairment due to decreases in female hormone levels following menopause. A resting-state functional magnetic resonance imaging (fMRI) study [22] reported that early postmenopausal women exhibited significantly increased functional connectivity with the insula, prefrontal cortex, and superior frontal cortex compared to premenopausal women when the amygdala was used as the seed region and suggested that these regions were related to depressive states, poor sleep quality, and decreased executive function. Another study [21] concerning task-related connectivity suggested that postmenopausal women showed increased connectivity between the left and right hippocampi during the verbal encoding task compared to premenopausal women. These studies exclusively explored a specific brain region of interest (ROI), either the hippocampus or amygdala. However, a functional connectivity study using a seed region with reduced volume in postmenopausal women has not been published yet.

A recent MRI study [24] reported that thalamic volume loss was one of the first signs of cognitive decline in

patients with early mild cognitive impairment (MCI). Cognitive decline is a frequent complaint during the transition to menopause in postmenopausal women [25]. The thalamus is an evolutionarily conserved structure with extensive reciprocal connections to cortical regions, and it plays an important role in learning and memory [26, 27]. A positron emission tomography (PET) study [28] reported that postmenopausal women receiving ET showed increased thalamic-basal ganglia connectivity compared to postmenopausal women without ET. To the best of our knowledge, no comparative neuroimaging study on alterations in the brain volume and functional connectivity, especially focusing on the thalamic subnuclei in premenopausal vs. postmenopausal women has been reported.

Thus, this study compared the brain volume changes in specialized with thalamic subnuclei, between the two groups, premenopausal and postmenopausal women. Also, the functional connectivity in targeted brain regions that are related with structural atrophy in postmenopausal women will be evaluated.

MATERIALS AND METHODS

Subjects

Twenty-one postmenopausal women (mean age: 55.3 ± 2.5 years) and 21 premenopausal women (mean age: 39.8 ± 7.6 years) underwent MRI. All women with right-handedness were recruited via advertisements.

The premenopausal group was selected based on several criteria [1]: 1) absence of a menopause diagnosis as determined by the Stages of Reproductive Aging Workshop (STRAW) +10 criteria; and 2) regular menstrual bleeding. Ovulation day was estimated using the rhythm method. Participants with a history of psychiatric or neurological illnesses were excluded. Those who had undergone any hormonal or steroid treatment and those who had used oral contraceptives in the month preceding the study were also excluded. We included 21 premenopausal women in the premenstrual phase, 10 to 19 days prior to their expected period.

The postmenopausal group was selected based on the following inclusion criteria [1, 29]: 1) those with a confirmed diagnosis of menopause according to STRAW +10 criteria; and 2) an absence of menstrual bleeding for more than one year. Participants who had a history of hysterectomy or bilateral oophorectomy were excluded. Those whose follicle-stimulating hormone (FSH) levels were less than $40 \mu\text{g/mL}$ were also excluded. Similar to the premenopausal group, those who had a history of neurological illnesses and those who had received hormonal or steroid treatments or used oral contraceptives

in the month prior to the study were excluded. The average duration since the onset of menopause in these women was 4.8 ± 2.5 years. In terms of demographics, the majority of the premenopausal women, 18 out of 21, were married with an average of 1.8 ± 1.0 children, while 3 were single. In contrast, all postmenopausal women were married with an average of 2.8 ± 0.7 children.

This study was approved by the Institutional Review Board (IRB) of Chonnam National University Hospital (IRB-CNUH). The experimental procedure was explained to all Participants and written informed consent was obtained. All experimental procedures and methods were performed in accordance with relevant guidelines and regulations approved by the IRB-CNUH.

Sex hormones

Levels of sex hormones including estradiol (E2), FSH, and luteinizing hormone (LH) were measured by chemiluminescent immunoassays using an ADVIA Centaur System (Bayer Healthcare, Chicago, IL, USA). Levels of estrogen, estriol (E3), free testosterone (free-T), and sex hormone-binding globulin (SHBG) were measured by radioimmunoassay using a gamma counter (Cobra 5010 Quantum, Packard Instrument Co, Meriden, CT, USA).

MRI data acquisition

MRI and fMRI images were collected on a 3.0-T Magnetom Tim Trio MR Scanner (Siemens Medical Solutions, Erlangen, Germany) with an 8-channel head coil. For structural imaging, T1-weighted sagittal images were acquired using a refined three-dimensional magnetization-prepared rapid-acquisition gradient echo (3D-MPRAGE) pulse sequence with the following parameters: a repetition time (TR) of 1900 ms and an echo time (TE) of 2.35 ms. The field of view (FOV) was maintained at 256×256 mm² with a matrix size of 256×256 . This protocol was designed to yield a comprehensive set of 176 slices per scan, with the number of excitations (NEX) set to 1.

Two 1-minute resting-state blood oxygen level-dependent (BOLD) scans were collected. These scans utilized a gradient echo-planar pulse sequence with the following parameters: a TR/TE of 2000 ms/30 ms, a flip angle of 90°, an FOV of 220×220 mm², and a matrix size of 64×64 . The slice gap was meticulously set to 0 mm to ensure contiguous coverage and optimal signal quality.

Data processing and analysis

Anatomical (surface area and subcortical volume) and resting-state functional MR data were post-processed

using FreeSurfer 6.0 software package (<http://surfer.nmr.mgh.harvard.edu>). Thalamic subnuclei were calculated using FreeSurfer 7.2 software package. Resting-state fMRI data analysis included runs with a temporal signal-to-noise ratio greater than 125 and a relative head motion value of less than 1 mm between one or more pairs of consecutive TRs [30].

Structural analysis

T1-weighted images were analyzed with the procedure described in our previous studies [30, 31]. We incorporated advanced motion correction techniques and intensity non-uniformity adjustments. Talairach transformation was performed for each subject's brain, followed by removal of non-brain tissues. We conducted a detailed segmentation for cortical gray matter, subcortical white matter, and deep gray matter volumetric structures [29, 30]. The cortical surface was reconstructed through triangular tessellation at the gray matter/white matter interface and the gray matter/cerebrospinal fluid boundary, followed by topological correction [29, 30].

Thirty brain regions of interest (ROIs) were selected from both hemispheres based on previous studies [1, 6, 19, 20, 32] focused on postmenopausal women, including the superior/middle/inferior frontal cortex, superior/middle/inferior temporal cortex, superior/inferior parietal lobule, lateral/medial orbitofrontal cortex, insula, hippocampus, thalamus, putamen, and amygdala. Twenty-three thalamic subnuclei (46 ROIs) were extracted for the left and right hemispheres, including the antero-ventral (AV), latero-dorsal (LD), lateral posterior (LP), ventral anterior (VA), ventral anterior magnocellular (VAmc), ventral lateral anterior (VL_a), ventral lateral posterior (VL_p), ventral posterolateral (VPL), central medial (CeM), central lateral (CL), paracentral (Pc), centromedian (CM), parafascicular (Pf), reuniens/medial ventral (MV-re), mediodorsal medial magnocellular (MD_m), mediodorsal lateral parvocellular (MD_l), lateral geniculate (LGN), medial geniculate (MGN), limitans/supragenulate (L-SG), pulvinar anterior (PuA), pulvinar medial (PuM), pulvinar lateral (PuL), and pulvinar inferior (PuI) (Figure 1) [29].

Resting-state fMRI analysis

Preprocessing of resting-state fMRI data was conducted using FS-FAST (the FreeSurfer Functional Analysis Stream) [30, 33]. First, functional data were realigned to correct for rigid head motion and corrected for slice time correction. These preprocessed functional data were then normalized to a common space (fsaverage). Normalized functional data were smoothed using a 3D Gaussian kernel (5-mm full-width-half-maximum). Spurious variance was reduced by nuisance regression derived from rigid body motion correction, signal regression in the

white matter and cerebrospinal fluid, and global signal regression [30]. Functional data underwent a specialized low-pass filtering process at 0.08 Hz, effectively isolating neural signals from physiological-related noise. Based on reduced cortical surface areas in postmenopausal women, we conducted a voxel-wise resting-state connectivity analysis using the left medial orbitofrontal cortex (mOFC), right lateral OFC (lOFC), and right superior temporal cortex (STC) as seed regions. Resting-state functional connectivity between the seed region and the whole brain was determined via multiple regression analysis of the average time-series in each voxel [30].

Statistical analyses

Demographic characteristics and sex hormones

Independent samples t-test was used to compare the age and sex hormone levels of the premenopausal and postmenopausal women using SPSS (version 28.0, IBM, Armonk, NY, USA).

Structural analysis

The Shapiro-Wilk test was used to assess the normality of the MR data. Multivariate analysis of variance, with age and whole brain volume as covariates, was used to compare cortical surface area and subcortical volume between the two groups. The significance level was set to 0.05 ($p < 0.0017$) after Bonferroni's correction for 30 ROIs to adjust for multiple comparisons. Multivariate analysis of

variance, with age and whole brain volume as covariates, was used to evaluate thalamic subnuclei volumes. The significance level was set to 0.05 ($p = 0.001$) after Bonferroni's correction for 46 ROIs. A Spearman's correlation test was used to evaluate the relationship between female sex hormone levels and surface area (or thalamic subnuclei volumes).

Resting-state fMRI analysis

Multivariate analysis of variance, with age as a covariate, was used to compare functional connectivity between the two groups, which was corrected for multiple comparisons with Monte Carlo simulation using a voxel height threshold of $p < 0.005$ with a cluster-wise p-value (CWP) threshold of $p < 0.05$ [30]. A partial correlation adjusted for age was used to evaluate the relationship between left OFC-right thalamus functional connectivity and female sex hormone levels.

RESULTS

Age and serum sex hormone levels

There was a significant difference in age between the 2 groups ($p < 0.001$). Postmenopausal women had lower total estrogen ($p < 0.001$) and E2 levels ($p < 0.001$) and higher FSH ($p < 0.001$) and LH levels ($p = 0.005$) than premenopausal women (Table 1). However, there were no significant differences in E3, free-T, or SHBG between the two groups ($p > 0.05$, Bonferroni-corrected; Table 1).

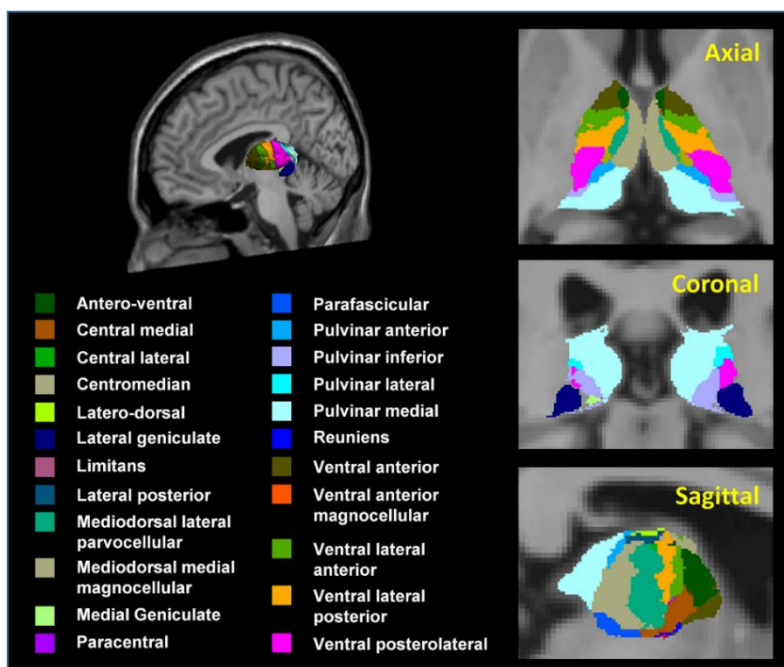


Figure 1. 3D atlas of the thalamus and its subnuclei segmentation. Segmentation of thalamic subnuclei was performed using a built-in module of FreeSurfer.

Table 1. Sex hormone levels in premenopausal and postmenopausal women.

	Premenopausal women (n=21)	Postmenopausal women (n=21)	p-value
Estrogen ^a (pg/mL)	566.8 ± 319.7	76.5 ± 40.9	< 0.001***
Estradiol (E2) ^b (pg/mL)	212.7 ± 159.9	14.4 ± 7.6	< 0.001***
Estriol (E3) ^c (pg/mL)	2.7 ± 1.4	2.3 ± 1.3	0.552
Free-testosterone ^d (pg/mL)	0.4 ± 0.3	0.2 ± 0.1	0.294
Sex hormone binding ^e -globulin (SHBG, nmol/L)	102.0 ± 33.3	70.7 ± 17.3	0.026*
Follicle-stimulating ^f hormone (FSH, mIU/mL)	6.1 ± 3.6	63.3 ± 21.5	< 0.001***
Luteinizing hormone ^g (LH, mIU/mL)	14.2 ± 14.2	36.5 ± 11.5	0.005**

Data are presented as the mean ± standard deviation (SD).

* $p < 0.05$, ** $p < 0.01$, *** $p < 0.001$.

Reference ranges for hormones in premenopausal and postmenopausal women ("Clinical Research Service" [GRQC-017 Rev.0] published in 2007 by Green Cross Reference Laboratory).

^aPremenopausal women, more than 61 pg/mL; postmenopausal women, less than 60 pg/mL.

^bPremenopausal women, 11 to 526 pg/mL; postmenopausal women, less than 37 pg/mL.

^cPregnant women, 49.2 to 375 ng/mL at 21 to 42 weeks.

^dWomen aged 20 to 39 years, 0.06 to 2.5 pg/mL; women aged 40 to 59 years, 0.04 to 2.0 pg/mL.

^eWomen, 16 to 120 nmol/L; men, 10 to 73 nmol/L.

^fPremenopausal women, 1.5 to 33.4 mIU/mL; postmenopausal women, 23 to 116.3 mIU/mL.

^gPremenopausal women, 0.5 to 73.6 mIU/mL; postmenopausal women, 15.9 to 54.0 mIU/mL.

Cortical surface area and subcortical volume

As shown in Figures 2, 3, the surface area of the left mOFC, right IOFC, and right STC was significantly reduced in postmenopausal women compared to premenopausal women ($p < 0.05$, Bonferroni-corrected; Table 2). None of the other 27 ROIs were significantly different between the two groups (all $p > 0.05$; Figure 3 and Table 2).

Although postmenopausal women did not show volume atrophy in the right thalamus, the volume of the right PuA, which is one of thalamic subnuclei, was significantly decreased ($p < 0.05$, Bonferroni-corrected; Figure 4 and Table 3). There was also a significant volume difference in the right PuA between the two groups (Mann-Whitney U-test; $p < 0.001$). None of the other 45 ROIs were significantly different between the two groups (all $p > 0.05$; Figure 4 and Table 3).

Correlation between structural changes and sex hormone levels

Estrogen levels were positively correlated with the surface area of the left mOFC ($p = 0.35$, $p = 0.041$), right STG ($p = 0.31$, $p = 0.045$), and right IOFC ($p = 0.41$, $p = 0.007$) and the volume of the right PuA ($p =$

0.32, $p = 0.037$), respectively (Figure 5). E2 levels were positively correlated with the surface area of the left mOFC ($p = 0.42$, $p = 0.006$) and right IOFC ($p = 0.40$, $p = 0.008$) and the volume of the right PuA ($p = 0.41$, $p = 0.008$), respectively (Figure 5). Note that no correlation between the E2 level and the surface area of the right STG was observed.

Functional connectivity analysis

Significantly lower functional connectivity between the left mOFC and right thalamus was found in postmenopausal women compared to premenopausal women ($p < 0.005$, Monte-Carlo corrected; Figure 6). However, no significant difference ($p > 0.005$) was detected in whole-brain connectivity of the other two ROIs (right IOFC or right STC) between the two groups.

DISCUSSION

Summary of main findings

In this study, postmenopausal women exhibited lower total estrogen and E2 levels and higher FSH and LH levels compared to premenopausal women. In the structural analysis, the surface areas of the left mOFC,

right IOFC, and right STC were significantly lower in postmenopausal women compared to premenopausal women. In addition, the functional connectivity between the left mOFC and the thalamus in postmenopausal

women was significantly lower than premenopausal women. Also, the volume of the right PuA, which is one of the important thalamic subnuclei, was significantly reduced in postmenopausal women compared to

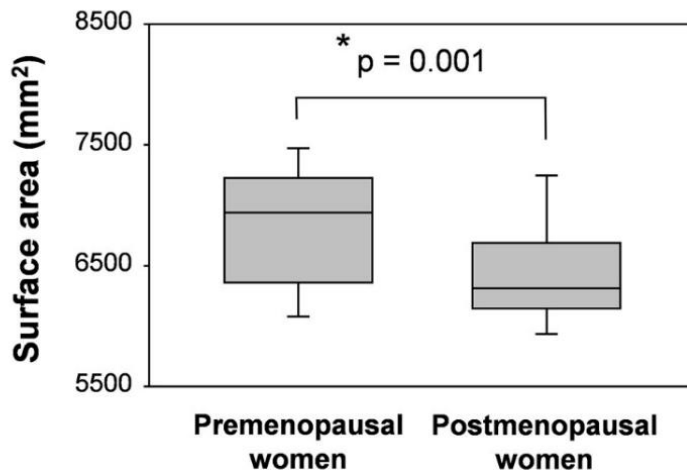
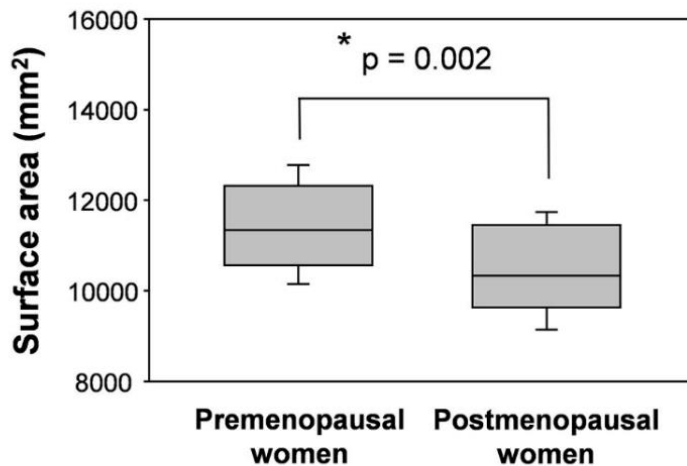
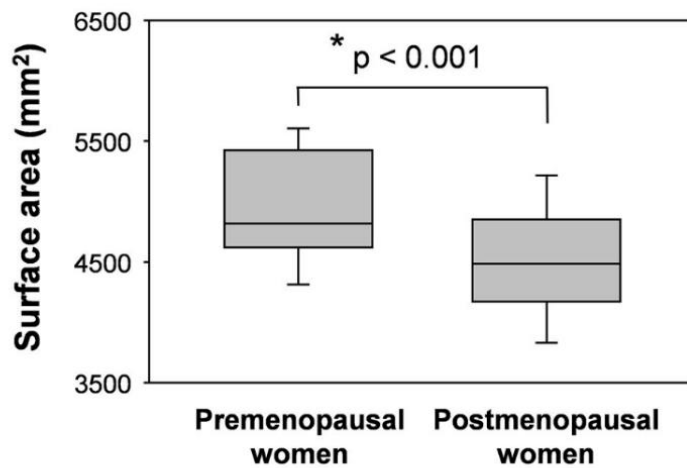
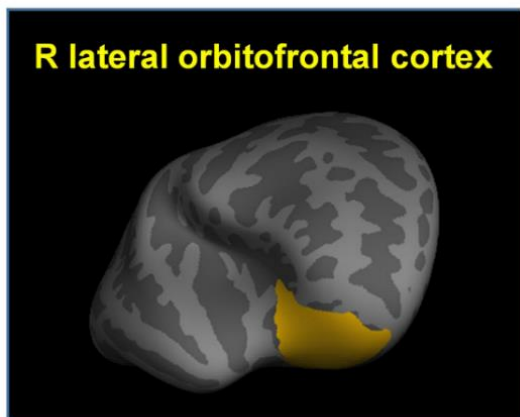
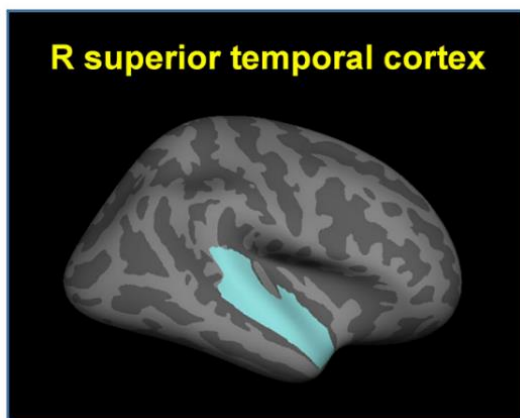
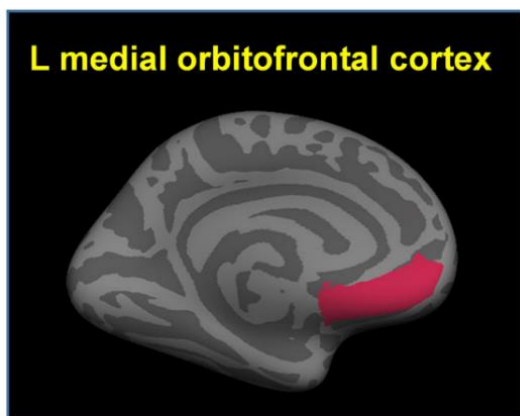


Figure 2. Reduced surface areas in postmenopausal women compared to premenopausal women. Postmenopausal women showed significantly reduced surface areas in the left medial orbitofrontal cortex (mOFC), right superior temporal cortex (STC), and right lateral orbitofrontal cortex (IOFC) compared to premenopausal women. *Meet Bonferroni-corrected significance level.

premenopausal women (Figure 4). Given that decreases in female sex hormones are considered as a sign of menopause [2, 9, 34], our findings suggest that diminished mOFC size in postmenopausal women is closely associated with the correspondent functional abnormalities.

Reduced surface areas in postmenopausal women

Postmenopausal women showed significantly lower levels of surface areas in the left mOFC and right IOFC compared to premenopausal women. The OFC is implicated in multiple cognitive processes, including inhibitory control, context memory, recency judgment, and behavior choice [35]. Decreases in female sex hormones following menopause may be linked to the left mOFC and right IOFC, further supporting the hypothesis that menopause-related hormonal changes can lead to alterations in brain morphology and cognitive dysfunction [10, 19]. The effects of estrogen on the structure of the prefrontal cortex, including the OFC, are relevant to the kinds of cognitive symptoms reported by women undergoing natural, medical, and surgical menopause [8, 32, 34, 36, 37]. The PFC has a relatively high density of estrogen receptors, and estrogen receptor mRNA is also highly expressed throughout the PFC [38–40]. A previous study [40] found a positive correlation between E2 levels and cortical thickness in the orbitofrontal cortex. In our study, the surface area of the left mOFC was positively correlated with estrogen and E2 levels, and the surface

area of the right IOFC was positively correlated with estrogen levels. A morphometric study [6] on ET found increased volume in the OFC of postmenopausal women receiving ET compared to postmenopausal women. A similar study [32] reported significantly lower gray matter concentrations in the bilateral orbitofrontal cortex of postmenopausal women receiving ET than in postmenopausal women without ET.

We found lower surface areas in the right STC of postmenopausal women than in premenopausal women. This finding is consistent with prior evidence reporting that the STC volume was positively correlated with female sex hormones [1]. The STC has been implicated in language processing and social perception and is widely recognized as being sensitive to estrogen changes [1, 37, 38]. Estrogen exposure was positively correlated with metabolism in the STC [41, 42]. Concerning the close connection between the estrogen level and STC volume, our findings support a potential role of decreases in sex hormones following menopause due to the correspondent brain structural atrophy. However, further study is needed to elucidate the specific cognitive and emotional implications in connection with these structural changes.

Functional connectivity between mOFC and thalamus

Together with the surface area analysis, we analysis revealed significantly decreased functional connectivity

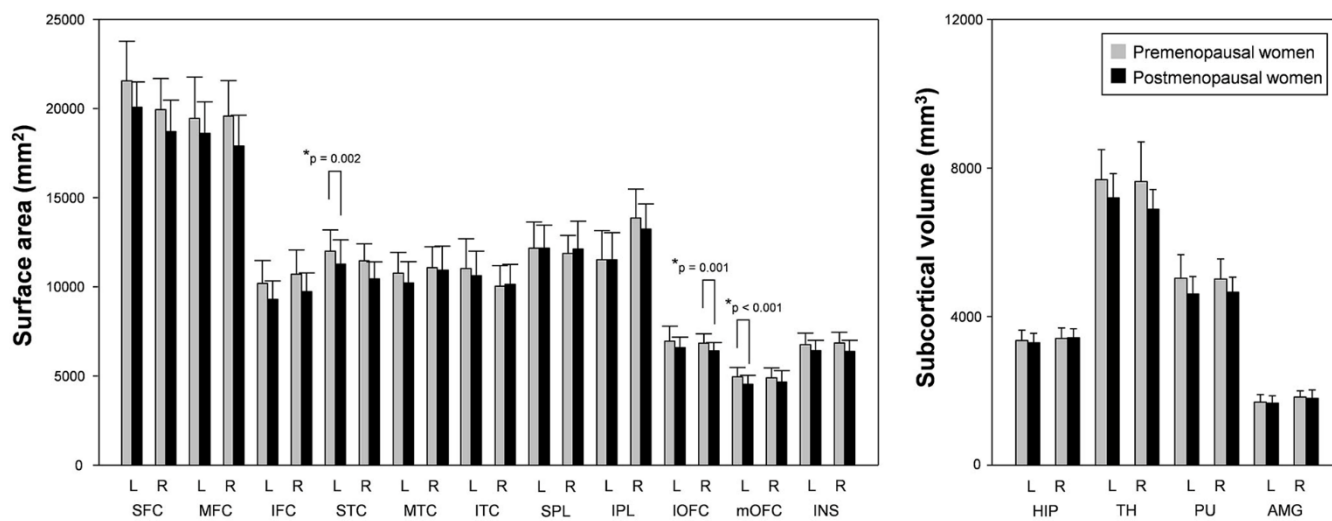


Figure 3. Surface areas and subcortical volumes in postmenopausal women and premenopausal women. Postmenopausal women showed significantly reduced surface areas of the left mOFC, right IOFC, and right STC compared to premenopausal women. L; left, R; right, SFC/MFC/IFC; superior/middle/inferior frontal cortex, STC/MTC/ITC; superior/middle/inferior temporal cortex, SPL/IPL; superior/inferior parietal lobule, IOFC/mOFC; lateral/medial orbitofrontal cortex, INS; insula, HIP; hippocampus, TH; thalamus, PU; putamen, AMG; amygdala. *Meet Bonferroni-corrected significance level.

Table 2. Comparison of brain volumes between premenopausal and postmenopausal women.

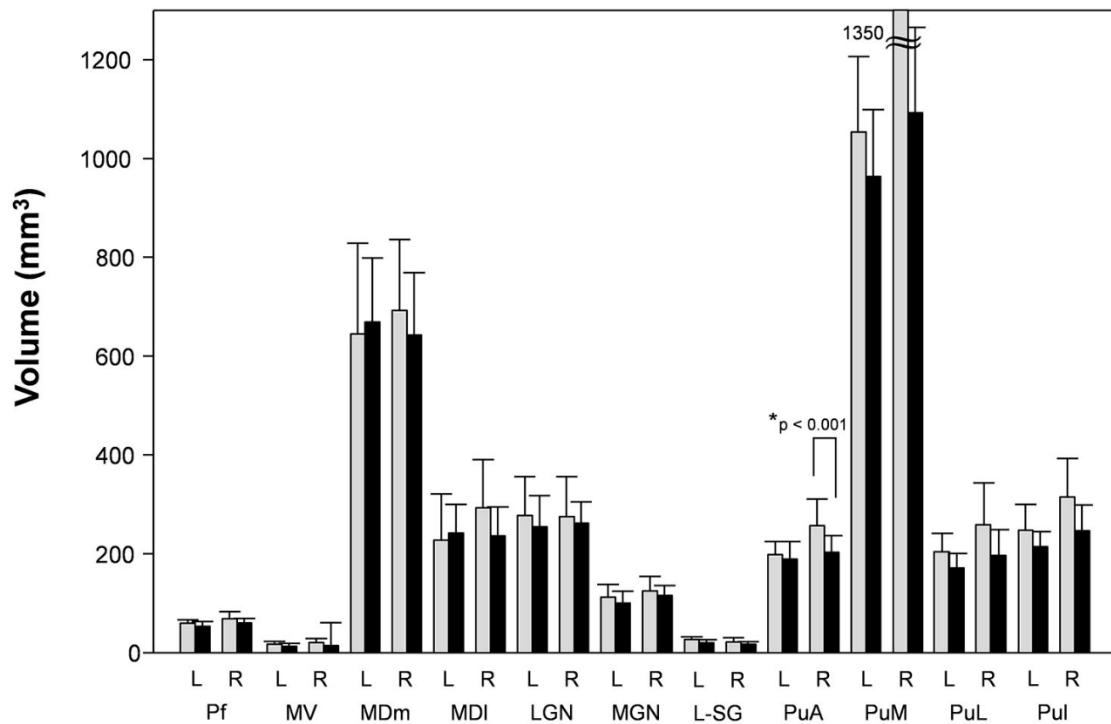
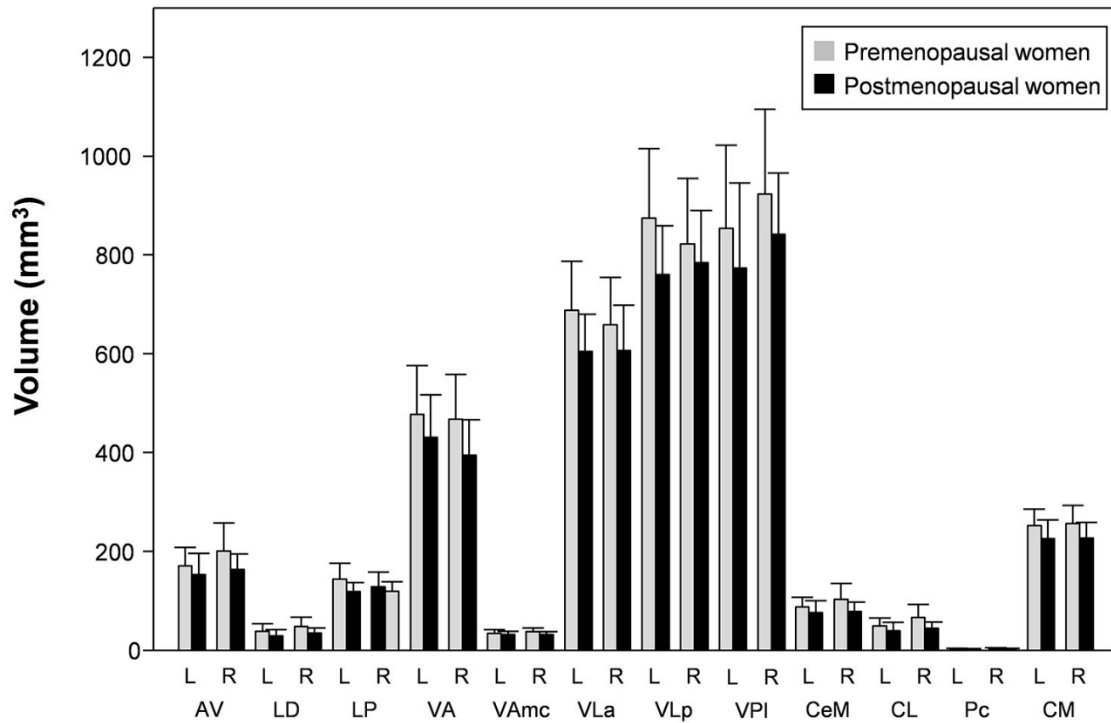
Brain regions	Abbrev.	Premenopausal women (n = 21)	Postmenopausal women (n = 21)	F-value	P-value	Cohen's d	Normality test (p-value)
<i>a. Surface area</i>							
L Superior frontal gyrus	SFC	21560.3 ± 2225.9	20069.9 ± 1428.8	10.8	0.002	1.04	0.116
R Superior frontal gyrus		19950.4 ± 1735.1	18708.3 ± 1771.7	6.4	0.016	0.80	0.431
L Middle frontal gyrus	MFC	19444.1 ± 2310.1	18616.8 ± 1763.5	5.2	0.028	0.72	0.853
R Middle frontal gyrus		19578.4 ± 1991.2	17918.5 ± 1714.8	9.8	0.003	0.99	0.963
L Inferior frontal gyrus	IFC	10190.0 ± 1287.9	9306.6 ± 1024.1	0.7	0.403	0.27	0.923
R Inferior frontal gyrus		10709.5 ± 1366.6	9732.0 ± 1051.9	2.3	0.136	0.48	0.061
L Superior temporal gyrus	STC	12008.4 ± 1188.2	11272.0 ± 1363.9	5.9	0.020	0.77	0.529
R Superior temporal gyrus		11458.0 ± 960.1	10460.8 ± 955.2	11.5	0.002	1.07	0.423
L Middle temporal gyrus	MTC	10768.6 ± 1174.2	10225.9 ± 1194.4	9.6	0.004	0.98	0.926
R Middle temporal gyrus		11071.5 ± 1192.0	10936.0 ± 1360.6	7.5	0.009	0.87	0.470
L Inferior temporal gyrus	ITC	11031.1 ± 1667.7	10630.0 ± 1377.7	8.0	0.007	0.89	0.007
R Inferior temporal gyrus		10039.0 ± 1152.8	10145. ± 1113.9	1.1	0.301	0.33	0.709
L Superior parietal lobule	SPL	12177.9 ± 1463.8	12172.3 ± 1303.0	0.6	0.452	0.25	0.857
R Superior parietal lobule		11882.0 ± 1013.5	12115.9 ± 1569.5	0.7	0.405	0.27	0.863
L Inferior parietal lobule	IPL	11520.5 ± 1642.0	11515.8 ± 1519.1	2.3	0.138	0.48	0.010
R Inferior parietal lobule		13858.1 ± 1635.6	13232.4 ± 1428.5	2.7	0.110	0.52	0.210
L Lateral orbitofrontal gyrus	IOFC	6969.0 ± 831.0	6596.4 ± 591.4	7.2	0.011	0.75	0.837
R Lateral orbitofrontal gyrus		6843.4 ± 525.4	6426.9 ± 450.6	12.5	0.001	1.12	0.131
L Medial orbitofrontal gyrus	mOFC	4972.3 ± 503.5	4540.3 ± 496.2	14.6	< 0.001*	0.21	0.412
R Medial orbitofrontal gyrus		4898.9 ± 550.9	4670.1 ± 624.7	5.1	0.030	0.71	0.014
L Insula	INS	6748.6 ± 647.5	6434.1 ± 580.0	4.7	0.037	0.69	0.889
R Insula		6856.9 ± 597.0	6384.4 ± 623.8	5.1	0.030	0.71	0.020
<i>b. Subcortical volume</i>							
L Hippocampus	HIP	3362.8 ± 277.5	3297.8 ± 249.0	2.4	0.130	0.49	0.988
R Hippocampus		3411.9 ± 284.4	3431.7 ± 236.9	0.5	0.479	0.22	0.375
L Thalamus	TH	7691.5 ± 804.2	7196.5 ± 655.6	1.8	0.192	0.42	0.096
R Thalamus		7637.2 ± 1065.0	6892.8 ± 529.4	6.0	0.019	0.78	0.012
L Putamen	PU	5037.3 ± 626.8	4611.9 ± 466.8	1.7	0.204	0.41	0.788
R Putamen		5013.4 ± 544.3	4651.1 ± 413.6	5.5	0.025	0.74	0.347
L Amygdala	AMG	1695.3 ± 206.9	1672.9 ± 192.4	1.1	0.310	0.33	0.013
R Amygdala		1834.4 ± 169.6	1804.0 ± 223.9	6.0	0.019	0.78	0.478

Multivariate analysis of variance, with age and whole brain volume as covariates, was used to compare surface size and subcortical volume between the two groups. Postmenopausal women showed significantly reduced surface areas in the left mOFG, right IOFG, and right STG compared to premenopausal women ($p < 0.05$, Bonferroni-corrected). Normality was evaluated by the Shapiro-Wilk test. L; left, R; right, abbrev; abbreviation.

*Meet Bonferroni-corrected significance level.

between the left mOFC and right thalamus in postmenopausal women compared to premenopausal women. This finding reinforces the hypothesis that the left orbitofrontal-bilateral thalamus connectivity is associated with cognitive impairment [43]. Several studies [44–46] demonstrated key roles for

orbitofrontal-thalamic connections in the occurrence and development of psychiatric symptoms and cognitive impairment. In addition, OFC has long been known to play a central role in female sex hormones. For example, a study [47] reported that activation of the OFC from sexually relevant stimuli was positively



Thalamic subnuclei

Figure 4. Thalamic subnuclei volumes in postmenopausal vs. premenopausal women. Postmenopausal women showed significantly reduced volume of the right PuA compared to premenopausal women. L; left, R; right, AV; antero-ventral, LD; latero-dorsal, LP; lateral posterior, VA; ventral anterior, VAMc; ventral anterior magnocellular, VLa; ventral lateral anterior, VLp; ventral lateral posterior, VPL; ventral posterolateral, CeM; central medial, CL; central lateral, Pc; paracentral, CM; centromedian, Pf; parafascicular, MV-re; reunions (medial ventral), MDm; mediodorsal medial magnocellular, MDI; mediodorsal lateral parvocellular, LGN; lateral geniculate, MGN; medial geniculate, L-SG; limitans (suprageniculate), PuA; pulvinar anterior, PuM; pulvinar medial, PuL; pulvinar lateral, Pul; pulvinar inferior. *Meet Bonferroni-corrected significance level.

Table 3. Comparison of thalamic subnuclei volumes between premenopausal and postmenopausal women.

Thalamic nuclei		Abbrev.	Premenopausal women	Postmenopausal women	F-value	P-value	Cohen's d	Normality test (p-value)
Anterior	L Anteroventral	AV	171.7 ± 37.7	153.5 ± 43.4	0.3	0.564	0.17	0.976
	R Anteroventral		201.6 ± 56.9	163.7 ± 32.1	2.4	0.128	0.49	0.217
Lateral	L Laterodorsal	LD	39.1 ± 14.9	30.2 ± 12.0	0.1	0.787	0.10	0.694
	R Laterodorsal		48.9 ± 19.0	36.0 ± 10.0	0.3	0.602	0.17	0.465
Ventral	L Laterodorsal posterior	LP	144.8 ± 31.8	118.9 ± 18.8	8.9	0.005	0.94	< 0.001
	R Laterodorsal posterior		129.0 ± 30.1	119.9 ± 19.9	0.0	0.960	0.00	0.988
	L Ventral anterior	VA	478.4 ± 98.5	431.3 ± 86.4	0.1	0.783	0.10	0.191
	R Ventral anterior		468.2 ± 90.6	394.9 ± 72.2	4.4	0.043	0.66	0.448
	L Ventral anterior magnocellular	VAmc	35.5 ± 6.8	32.7 ± 6.3	0.2	0.681	0.14	0.250
	R Ventral anterior magnocellular		38.4 ± 7.6	33.0 ± 5.8	2.8	0.100	0.53	0.108
Intralaminar	L Ventral lateral anterior	VLa	688.9 ± 99.2	605.5 ± 75.0	8.5	0.006	0.92	0.026
	R Ventral lateral anterior		659.6 ± 95.8	607.1 ± 91.8	2.9	0.099	0.54	0.174
	L Ventral lateral posterior	VLp	875.4 ± 140.5	761.0 ± 98.6	10.7	0.002	1.03	0.043
	R Ventral lateral posterior		823.3 ± 132.5	785.3 ± 105.6	2.0	0.165	0.45	0.643
	L Ventral posterolateral	VPL	854.6 ± 168.0	774.2 ± 172.3	3.0	0.090	0.55	0.226
	R Ventral posterolateral		924.1 ± 171.7	842.8 ± 124.0	2.4	0.130	0.49	0.961
	L Central medial	CeM	87.9 ± 20.0	76.4 ± 24.4	0.1	0.712	0.10	0.724
	R Central medial		104.0 ± 32.0	79.3 ± 18.8	3.3	0.076	0.57	0.032
	L Central lateral	CL	50.0 ± 16.0	40.6 ± 16.7	0.0	0.850	0.00	0.548
	R Central lateral		67.2 ± 26.8	45.3 ± 12.8	1.7	0.198	0.41	0.009
L Paracentral	Pc	4.0 ± 0.6	3.6 ± 0.8	0.9	0.347	0.30	0.044	
R Paracentral		4.9 ± 1.0	4.2 ± 0.5	2.8	0.101	0.53	0.008	
L Centromedian	CM	253.3 ± 33.2	227.1 ± 37.8	2.4	0.128	0.49	0.300	
R Centromedian		256.9 ± 37.2	227.5 ± 32.1	3.1	0.086	0.56	0.468	
L Parafascicular	Pf	60.8 ± 7.0	54.4 ± 10.4	2.8	0.104	0.53	0.612	
R Parafascicular		70.6 ± 13.8	61.3 ± 9.7	2.3	0.139	0.48	0.016	
Medial	L Reuniens (medial ventral)	MV-re	18.5 ± 5.8	14.2 ± 5.7	0.4	0.543	0.20	0.293
	R Reuniens (medial ventral)		22.3 ± 8.1	15.1 ± 4.7	2.9	0.097	0.54	0.018
	L Mediodorsal medial magnocellular	MDm	645.8 ± 184.5	670.0 ± 130.2	3.2	0.081	0.57	< 0.001
	R Mediodorsal medial magnocellular		694.2 ± 143.4	644.5 ± 125.7	9.5	0.004	0.98	0.680
	L Mediodorsal lateral parvocellular	MDl	228.7 ± 93.5	243.5 ± 58.0	3.9	0.056	0.62	< 0.001
	R Mediodorsal lateral parvocellular		295.0 ± 96.9	237.6 ± 58.6	10.7	0.002	1.03	0.170
Posterior	L Lateral geniculate	LGN	279.3 ± 78.1	256.5 ± 62.9	0.3	0.567	0.17	0.496
	R Lateral geniculate		276.6 ± 81.2	263.7 ± 42.9	0.2	0.653	0.14	0.361
	L Medial Geniculate	MGN	113.5 ± 26.1	101.4 ± 24.1	0.9	0.358	0.30	0.370
	R Medial Geniculate		126.5 ± 29.3	117.1 ± 20.0	1.1	0.299	0.33	0.901
	L Limitans (suprageniculate)	L-SG	28.4 ± 5.2	21.1 ± 6.2	8.3	0.006	0.91	0.768
	R Limitans (suprageniculate)		23.3 ± 8.3	18.5 ± 5.4	0.8	0.390	0.28	0.004
	L Pulvinar anterior	PuA	199.7 ± 26.6	190.9 ± 35.2	0.4	0.508	0.20	0.215
	R Pulvinar anterior		258.1 ± 54.4	204.4 ± 34.1	16.2	< 0.001*	1.27	0.029
	L Pulvinar medial	PuM	1055.3 ± 152.6	964.3 ± 135.9	0.0	0.885	0.00	0.187
	R Pulvinar medial		1350.8 ± 272.4	1094.0 ± 172.5	8.7	0.005	0.93	0.025
	L Pulvinar lateral	PuL	205.8 ± 36.8	172.5 ± 29.9	4.7	0.036	0.69	0.306
	R Pulvinar lateral		260.0 ± 84.8	198.4 ± 52.5	5.7	0.022	0.76	0.008
	L Pulvinar inferior	PuI	249.2 ± 52.2	216.3 ± 30.2	0.1	0.780	0.10	0.136
	R Pulvinar inferior		316.3 ± 78.4	248.3 ± 52.2	2.6	0.118	0.51	0.069

Multivariate analysis of variance, with age and whole brain volume as covariates, was used to compare thalamic subnuclei volumes between the two groups. Postmenopausal women showed significantly reduced volume in the right PuA compared to premenopausal women ($p < 0.05$, Bonferroni-corrected). Normality was evaluated by the Shapiro-Wilk test. L; left, R; right, abbrev; abbreviation. *Meet Bonferroni-corrected significance level.

correlated with the estradiol-to-progesterone ratio in women. Also, other studies [8, 48] demonstrated positive correlations between ET and brain activity in the OFC during emotion identification tasks and negative emotional image presentations, which suggests a potential link between the OFC and female sex hormones. Diminished OFC size and functional connectivity in postmenopausal women may be associated with cognitive dysfunction caused by

reduced sex hormone levels in connection with neurophysiological change following menopause.

Decreased thalamic subnuclei volume

Although postmenopausal women did not show volume atrophy in the right thalamus, the volume of right PuA, which is one of thalamic subnuclei, was significantly decreased. In addition, the volume of the right PuA was

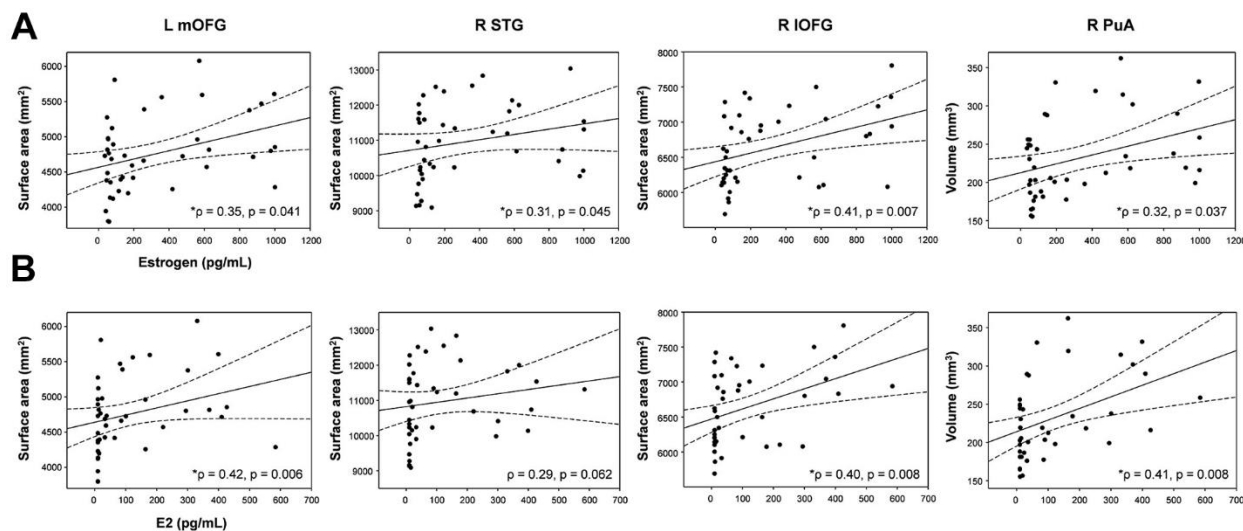


Figure 5. Correlations between brain structural changes and female sex hormone levels. (A) Estrogen levels were positively correlated with the surface areas of the left mOFC ($\rho = 0.35$, $p = 0.041$), right STG ($\rho = 0.31$, $p = 0.045$), and right IOFG ($\rho = 0.41$, $p = 0.007$) and the volume of the right PuA ($\rho = 0.32$, $p = 0.037$), respectively. (B) E2 levels were positively correlated with the surface area of the left mOFC ($\rho = 0.42$, $p = 0.006$) and right IOFG ($\rho = 0.40$, $p = 0.008$) and the volume of the right PuA ($\rho = 0.41$, $p = 0.008$), respectively. The dotted lines show 95% confidence intervals. L; left, R; right, mOFC; medial orbitofrontal cortex, STG; superior temporal cortex, IOFG; lateral orbitofrontal cortex, PuA; pulvinar anterior.

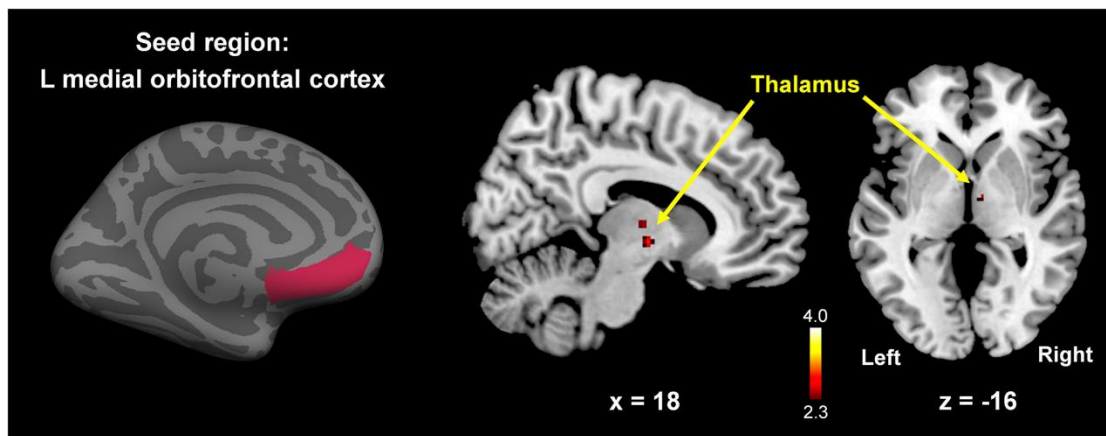


Figure 6. Between-group comparison map (premenopausal women vs. postmenopausal women) of the left mOFC functional connectivity. Postmenopausal women showed significantly lower functional connectivity between the left mOFC and right thalamus compared to premenopausal women ($p < 0.005$, Monte-Carlo corrected). The color-coded pixels were scaled to the range (t-value) more than the cut-off threshold ($p < 0.005$).

positively correlated with E2 levels. Although the association between cognitive function and estrogen in postmenopausal women is well known, little is known about thalamic subnuclei volumes. The thalamus, with its cortical and subcortical connections, is a critical node in networks supporting cognitive functions known to decline in normal aging [49]. Conversion from MCI to AD dementia was associated with reduced gray matter volume in the right thalamus, suggesting an association with worse cognitive performance [24]. Decreased left mOFC-right thalamus functional connectivity in postmenopausal women may affect specific thalamic subnuclei volumes, such as the PuA. Specifically, the pulvinar is a thalamic nucleus, which has long been considered a key structure for sensory processing and attention [50]. There is another evidence on morphological change of the PuA in patients with attention-deficit disorder [51]. Decreased PuA volume in postmenopausal women is closely related to decreases in female sex hormone levels following menopause. Our findings provide novel insight into the structural and functional changes in the brain associated with menopause.

Limitations and future directions

This study had some limitations. Firstly, our sample size was relatively small, with only 21 postmenopausal women included in the study. This small sample size may limit the generalizability of our findings and potentially introduce bias. To overcome this limitation, we used multiple-comparison correction to analyze brain volumes between the two groups. Secondly, our study groups were not matched for age, probably bringing about age-related volume alterations. Our findings should be interpreted cautiously because of the limitations related to age differences and the statistical methods used. Future studies should consider matching participants for age to control the potential effects of aging on brain volume and functional connectivity. Lastly, our study did not include a cognitive test to assess the cognitive abilities of the subjects. Given that menopause and the associated decreases in sex hormone levels have been linked to cognitive decline, the inclusion of cognitive testing would provide a more comprehensive understanding of the relationship between menopause, brain structure and function, and cognitive ability. Future research should incorporate cognitive assessments to elucidate the potential cognitive implications of the observed structural and functional brain changes in postmenopausal women.

CONCLUSIONS

Postmenopausal women showed significantly lower left mOFC, right IOFC, and right STC surface areas, reduced right PuA volume, and decreased left mOFC-right thalamus functional connectivity compared to pre-

menopausal women. If replicated in an independent sample, these findings will be helpful for understanding the effects of menopause on the altered brain volume and functional connectivity in postmenopausal women.

AUTHOR CONTRIBUTIONS

The first author Gwang-Won Kim was responsible for design of the study, data collection, data analysis, and article drafting. Kwangsung Park and Yun-Hyeon Kim performed the majority of experiments and interpretation of results. The corresponding author Gwang-Woo Jeong participated in the design of the study, data collection, data analysis, and article drafting and has approved the final manuscript and completed manuscript.

CONFLICTS OF INTEREST

The authors declare that they have no conflicts of interest.

ETHICAL STATEMENT AND CONSENT

The study involving human participants were reviewed and approved by the Institutional Review Board of Chonnam National University Hospital (IRB CNUH-2008-05-065). The patients/participants provided their written informed consent to participate in this study.

FUNDING

This research was supported by the grants from the National Research Foundation funded by the Korea government (MSIT; 2021R1C1C2011748 and 2022R1A2C2007809).

REFERENCES

1. Kim GW, Park K, Jeong GW. Effects of Sex Hormones and Age on Brain Volume in Post-Menopausal Women. *J Sex Med.* 2018; 15:662–70. <https://doi.org/10.1016/j.jsxm.2018.03.006> PMID:29628218
2. Davis SR, Lambrinoudaki I, Lumsden M, Mishra GD, Pal L, Rees M, Santoro N, Simoncini T. Menopause. *Nat Rev Dis Primers.* 2015; 1:15004. <https://doi.org/10.1038/nrdp.2015.4> PMID:27188659
3. Blagosklonny MV. Are menopause, aging and prostate cancer diseases? *Aging (Albany NY).* 2023; 15:298–307. <https://doi.org/10.18632/aging.204499> PMID:36707068
4. Yureneva S, Averkova V, Silachev D, Donnikov A, Gavisova A, Serov V, Sukhikh G. Searching for female

- reproductive aging and longevity biomarkers. *Aging* (Albany NY). 2021; 13:16873–94.
<https://doi.org/10.18632/aging.203206>
PMID:[34156973](https://pubmed.ncbi.nlm.nih.gov/34156973/)
5. Dubal DB, Wise PM. Neuroprotective effects of estradiol in middle-aged female rats. *Endocrinology*. 2001; 142:43–8.
<https://doi.org/10.1210/endo.142.1.7911>
PMID:[11145565](https://pubmed.ncbi.nlm.nih.gov/11145565/)
 6. Boccardi M, Ghidoni R, Govoni S, Testa C, Benussi L, Bonetti M, Binetti G, Frisoni GB. Effects of hormone therapy on brain morphology of healthy postmenopausal women: a Voxel-based morphometry study. *Menopause*. 2006; 13:584–91.
<https://doi.org/10.1097/01.gme.0000196811.88505.10> PMID:[16837880](https://pubmed.ncbi.nlm.nih.gov/16837880/)
 7. Li M, Lin J, Liang S, Chen Z, Bai Y, Long X, Huang S, Mo Z. The role of age at menarche and age at menopause in Alzheimer’s disease: evidence from a bidirectional mendelian randomization study. *Aging* (Albany NY). 2021; 13:19722–49.
<https://doi.org/10.18632/aging.203384>
PMID:[34347623](https://pubmed.ncbi.nlm.nih.gov/34347623/)
 8. Epperson CN, Amin Z, Ruparel K, Gur R, Loughead J. Interactive effects of estrogen and serotonin on brain activation during working memory and affective processing in menopausal women. *Psychoneuroendocrinology*. 2012; 37:372–82.
<https://doi.org/10.1016/j.psyneuen.2011.07.007>
PMID:[21820247](https://pubmed.ncbi.nlm.nih.gov/21820247/)
 9. McEwen B. Estrogen actions throughout the brain. *Recent Prog Horm Res*. 2002; 57:357–84.
<https://doi.org/10.1210/rp.57.1.357> PMID:[12017552](https://pubmed.ncbi.nlm.nih.gov/12017552/)
 10. Amin Z, Canli T, Epperson CN. Effect of estrogen-serotonin interactions on mood and cognition. *Behav Cogn Neurosci Rev*. 2005; 4:43–58.
<https://doi.org/10.1177/1534582305277152>
PMID:[15886402](https://pubmed.ncbi.nlm.nih.gov/15886402/)
 11. Suzuki S, Brown CM, Wise PM. Neuroprotective effects of estrogens following ischemic stroke. *Front Neuroendocrinol*. 2009; 30:201–11.
<https://doi.org/10.1016/j.yfrne.2009.04.007>
PMID:[19401209](https://pubmed.ncbi.nlm.nih.gov/19401209/)
 12. Hao J, Rapp PR, Leffler AE, Leffler SR, Janssen WG, Lou W, McKay H, Roberts JA, Wearne SL, Hof PR, Morrison JH. Estrogen alters spine number and morphology in prefrontal cortex of aged female rhesus monkeys. *J Neurosci*. 2006; 26:2571–8.
<https://doi.org/10.1523/JNEUROSCI.3440-05.2006>
PMID:[16510735](https://pubmed.ncbi.nlm.nih.gov/16510735/)
 13. Kramár EA, Chen LY, Brandon NJ, Rex CS, Liu F, Gall CM, Lynch G. Cytoskeletal changes underlie estrogen’s acute effects on synaptic transmission and plasticity. *J Neurosci*. 2009; 29:12982–93.
<https://doi.org/10.1523/JNEUROSCI.3059-09.2009>
PMID:[19828812](https://pubmed.ncbi.nlm.nih.gov/19828812/)
 14. Scharfman HE, MacLusky NJ. Estrogen and brain-derived neurotrophic factor (BDNF) in hippocampus: complexity of steroid hormone-growth factor interactions in the adult CNS. *Front Neuroendocrinol*. 2006; 27:415–35.
<https://doi.org/10.1016/j.yfrne.2006.09.004>
PMID:[17055560](https://pubmed.ncbi.nlm.nih.gov/17055560/)
 15. Cybulska AM, Rachubińska K, Szkup M, Schneider-Matyka D, Baranowska-Bosiacka I, Chlubek D, Lubkowska A, Panczyk M, Sołek-Pastuszka J, Grochans E. Serum levels of proinflammatory cytokines and selected bioelements in perimenopausal women with regard to body mass index. *Aging* (Albany NY). 2021; 13:25025–37.
<https://doi.org/10.18632/aging.203754>
PMID:[34890370](https://pubmed.ncbi.nlm.nih.gov/34890370/)
 16. Rodrigues MA, Foster JK, Verdile G, Joesbury K, Prince R, Devine A, Mehta P, Beilby J, Martins RN. Predicting memory decline as a risk factor for Alzheimer’s disease in older post-menopausal women: quod erat demonstrandum? *Int Psychogeriatr*. 2010; 22:332–5.
<https://doi.org/10.1017/S1041610209991190>
PMID:[19814842](https://pubmed.ncbi.nlm.nih.gov/19814842/)
 17. Mosconi L, Rahman A, Diaz I, Wu X, Scheyer O, Hristov HW, Vallabhajosula S, Isaacson RS, de Leon MJ, Brinton RD. Increased Alzheimer’s risk during the menopause transition: A 3-year longitudinal brain imaging study. *PLoS One*. 2018; 13:e0207885.
<https://doi.org/10.1371/journal.pone.0207885>
PMID:[30540774](https://pubmed.ncbi.nlm.nih.gov/30540774/)
 18. Erickson KI, Colcombe SJ, Raz N, Korol DL, Scalf P, Webb A, Cohen NJ, McAuley E, Kramer AF. Selective sparing of brain tissue in postmenopausal women receiving hormone replacement therapy. *Neurobiol Aging*. 2005; 26:1205–13.
<https://doi.org/10.1016/j.neurobiolaging.2004.11.009>
PMID:[15917105](https://pubmed.ncbi.nlm.nih.gov/15917105/)
 19. Kim TH, Kim B, Kim YR, Jeong CW, Lee YH. Gray matter differences associated with menopausal hormone therapy in menopausal women: a DARTEL-based VBM study. *Sci Rep*. 2023; 13:1401.
<https://doi.org/10.1038/s41598-023-28673-2>
PMID:[36697505](https://pubmed.ncbi.nlm.nih.gov/36697505/)
 20. Goto M, Abe O, Miyati T, Inano S, Hayashi N, Aoki S, Mori H, Kabasawa H, Ino K, Yano K, Iida K, Mima K, Ohtomo K. 3 Tesla MRI detects accelerated hippocampal volume reduction in postmenopausal women. *J Magn Reson Imaging*. 2011; 33:48–53.
<https://doi.org/10.1002/jmri.22328> PMID:[21182120](https://pubmed.ncbi.nlm.nih.gov/21182120/)

21. Jacobs EG, Weiss BK, Makris N, Whitfield-Gabrieli S, Buka SL, Klibanski A, Goldstein JM. Impact of Sex and Menopausal Status on Episodic Memory Circuitry in Early Midlife. *J Neurosci*. 2016; 36:10163–73. <https://doi.org/10.1523/JNEUROSCI.0951-16.2016> PMID:[27683911](https://pubmed.ncbi.nlm.nih.gov/27683911/)
22. Zhang S, Hu J, Fan W, Liu B, Wen L, Wang G, Gong M, Yang C, Zhang D. Aberrant Cerebral Activity in Early Postmenopausal Women: A Resting-State Functional Magnetic Resonance Imaging Study. *Front Cell Neurosci*. 2018; 12:454. <https://doi.org/10.3389/fncel.2018.00454> PMID:[30534056](https://pubmed.ncbi.nlm.nih.gov/30534056/)
23. Vega JN, Zurkovsky L, Albert K, Melo A, Boyd B, Dumas J, Woodward N, McDonald BC, Saykin AJ, Park JH, Naylor M, Newhouse PA. Altered Brain Connectivity in Early Postmenopausal Women with Subjective Cognitive Impairment. *Front Neurosci*. 2016; 10:433. <https://doi.org/10.3389/fnins.2016.00433> PMID:[27721740](https://pubmed.ncbi.nlm.nih.gov/27721740/)
24. van de Mortel LA, Thomas RM, van Wingen GA, and Alzheimer's Disease Neuroimaging Initiative. Grey Matter Loss at Different Stages of Cognitive Decline: A Role for the Thalamus in Developing Alzheimer's Disease. *J Alzheimers Dis*. 2021; 83:705–20. <https://doi.org/10.3233/JAD-210173> PMID:[34366336](https://pubmed.ncbi.nlm.nih.gov/34366336/)
25. Sliwinski JR, Johnson AK, Elkins GR. Memory Decline in Peri- and Post-menopausal Women: The Potential of Mind-Body Medicine to Improve Cognitive Performance. *Integr Med Insights*. 2014; 9:17–23. <https://doi.org/10.4137/IMI.S15682> PMID:[25125972](https://pubmed.ncbi.nlm.nih.gov/25125972/)
26. Kim GW, Park SE, Park K, Jeong GW. White Matter Connectivity and Gray Matter Volume Changes Following Donepezil Treatment in Patients With Mild Cognitive Impairment: A Preliminary Study Using Probabilistic Tractography. *Front Aging Neurosci*. 2021; 12:604940. <https://doi.org/10.3389/fnagi.2020.604940> PMID:[33796017](https://pubmed.ncbi.nlm.nih.gov/33796017/)
27. Nakajima M, Halassa MM. Thalamic control of functional cortical connectivity. *Curr Opin Neurobiol*. 2017; 44:127–31. <https://doi.org/10.1016/j.conb.2017.04.001> PMID:[28486176](https://pubmed.ncbi.nlm.nih.gov/28486176/)
28. Kenna HA, Rasgon NL, Geist C, Small G, Silverman D. Thalamo-Basal Ganglia connectivity in postmenopausal women receiving estrogen therapy. *Neurochem Res*. 2009; 34:234–7. <https://doi.org/10.1007/s11064-008-9756-z> PMID:[18535904](https://pubmed.ncbi.nlm.nih.gov/18535904/)
29. Kim GW, Park K, Jeong GW. Early Detection of Alzheimer's Disease in Postmenopausal Women Using Thalamic Subnuclear Volumetry. *J Clin Med*. 2023; 12:6844. <https://doi.org/10.3390/jcm12216844> PMID:[37959308](https://pubmed.ncbi.nlm.nih.gov/37959308/)
30. Kim GW, Farabaugh AH, Vetterman R, Holmes A, Nyer M, Nasirivanaki Z, Fava M, Holt DJ. Diminished frontal pole size and functional connectivity in young adults with high suicidality. *J Affect Disord*. 2022; 310:484–92. <https://doi.org/10.1016/j.jad.2022.04.069> PMID:[35427718](https://pubmed.ncbi.nlm.nih.gov/35427718/)
31. Kim GW, Park K, Kim YH, Jeong GW. Increased Hippocampal-Inferior Temporal Gyrus White Matter Connectivity following Donepezil Treatment in Patients with Early Alzheimer's Disease: A Diffusion Tensor Probabilistic Tractography Study. *J Clin Med*. 2023; 12:967. <https://doi.org/10.3390/jcm12030967> PMID:[36769615](https://pubmed.ncbi.nlm.nih.gov/36769615/)
32. Robertson D, Craig M, van Amelsvoort T, Daly E, Moore C, Simmons A, Whitehead M, Morris R, Murphy D. Effects of estrogen therapy on age-related differences in gray matter concentration. *Climacteric*. 2009; 12:301–9. <https://doi.org/10.1080/13697130902730742> PMID:[19415541](https://pubmed.ncbi.nlm.nih.gov/19415541/)
33. Zapetis SL, Nasirivanaki Z, Luther L, Holt DJ. Neural Correlates of Variation in Personal Space and Social Functioning in Schizophrenia and Healthy Individuals. *Schizophr Bull*. 2022; 48:1075–84. <https://doi.org/10.1093/schbul/sbac052> PMID:[35661903](https://pubmed.ncbi.nlm.nih.gov/35661903/)
34. Shanmugan S, Epperson CN. Estrogen and the prefrontal cortex: towards a new understanding of estrogen's effects on executive functions in the menopause transition. *Hum Brain Mapp*. 2014; 35:847–65. <https://doi.org/10.1002/hbm.22218> PMID:[23238908](https://pubmed.ncbi.nlm.nih.gov/23238908/)
35. Llorens A, Funderud I, Blenkmann AO, Lubell J, Foldal M, Leske S, Huster R, Meling TR, Knight RT, Solbakk AK, Endestad T. Preservation of Interference Effects in Working Memory After Orbitofrontal Damage. *Front Hum Neurosci*. 2020; 13:445. <https://doi.org/10.3389/fnhum.2019.00445> PMID:[31998097](https://pubmed.ncbi.nlm.nih.gov/31998097/)
36. Almey A, Cannell E, Bertram K, Filardo E, Milner TA, Brake WG. Medial prefrontal cortical estradiol rapidly alters memory system bias in female rats: ultrastructural analysis reveals membrane-associated estrogen receptors as potential mediators. *Endocrinology*. 2014; 155:4422–32. <https://doi.org/10.1210/en.2014-1463> PMID:[25211590](https://pubmed.ncbi.nlm.nih.gov/25211590/)

37. Maki PM, Resnick SM. Longitudinal effects of estrogen replacement therapy on PET cerebral blood flow and cognition. *Neurobiol Aging*. 2000; 21:373–83.
[https://doi.org/10.1016/s0197-4580\(00\)00123-8](https://doi.org/10.1016/s0197-4580(00)00123-8)
PMID:10867223
38. Signorelli SS, Sciacchitano S, Di Pino L, Costa MP, Pennisi G, Caschetto S. Effects of long-term hormone replacement therapy on arterial wall thickness, lipids and lipoproteins, fibrinogen and antithrombin III. *Gynecol Endocrinol*. 2001; 15:367–72.
<https://doi.org/10.1080/gye.15.5.367.372>
PMID:11727359
39. Perlman WR, Matsumoto M, Beltaifa S, Hyde TM, Saunders RC, Webster MJ, Rubinow DR, Kleinman JE, Weickert CS. Expression of estrogen receptor alpha exon-deleted mRNA variants in the human and non-human primate frontal cortex. *Neuroscience*. 2005; 134:81–95.
<https://doi.org/10.1016/j.neuroscience.2005.03.055>
PMID:15964702
40. Petersen N, Touroutoglou A, Andreano JM, Cahill L. Oral contraceptive pill use is associated with localized decreases in cortical thickness. *Hum Brain Mapp*. 2015; 36:2644–54.
<https://doi.org/10.1002/hbm.22797> PMID:25832993
41. Silverman DH, Geist CL, Kenna HA, Williams K, Wroolie T, Powers B, Brooks J, Rasgon NL. Differences in regional brain metabolism associated with specific formulations of hormone therapy in postmenopausal women at risk for AD. *Psychoneuroendocrinology*. 2011; 36:502–13.
<https://doi.org/10.1016/j.psyneuen.2010.08.002>
PMID:20810219
42. Smith YR, Minoshima S, Kuhl DE, Zubieta JK. Effects of long-term hormone therapy on cholinergic synaptic concentrations in healthy postmenopausal women. *J Clin Endocrinol Metab*. 2001; 86:679–84.
<https://doi.org/10.1210/jcem.86.2.7222>
PMID:11158031
43. Kim K, Kim SW, Myung W, Han CE, Fava M, Mischoulon D, Papakostas GI, Seo SW, Cho H, Seong JK, Jeon HJ. Reduced orbitofrontal-thalamic functional connectivity related to suicidal ideation in patients with major depressive disorder. *Sci Rep*. 2017; 7:15772.
<https://doi.org/10.1038/s41598-017-15926-0>
PMID:29150619
44. Xu X, Luo S, Wen X, Wang X, Yin J, Luo X, He B, Liang C, Xiong S, Zhu D, Fu J, Lv D, Dai Z, et al. Genetic Contribution of Synapse-Associated Protein 97 to Orbitofrontal-Striatal-Thalamic Circuitry Connectivity Changes in First-Episode Schizophrenia. *Front Psychiatry*. 2021; 12:691007.
<https://doi.org/10.3389/fpsy.2021.691007>
PMID:34349683
45. Silbersweig DA, Stern E, Frith C, Cahill C, Holmes A, Grootenk S, Seaward J, McKenna P, Chua SE, Schnorr L. A functional neuroanatomy of hallucinations in schizophrenia. *Nature*. 1995; 378:176–9.
<https://doi.org/10.1038/378176a0>
PMID:7477318
46. Murray GK, Cheng F, Clark L, Barnett JH, Blackwell AD, Fletcher PC, Robbins TW, Bullmore ET, Jones PB. Reinforcement and reversal learning in first-episode psychosis. *Schizophr Bull*. 2008; 34:848–55.
<https://doi.org/10.1093/schbul/sbn078>
PMID:18628272
47. Rupp HA, James TW, Ketterson ED, Sengelaub DR, Janssen E, Heiman JR. Neural activation in the orbitofrontal cortex in response to male faces increases during the follicular phase. *Horm Behav*. 2009; 56:66–72.
<https://doi.org/10.1016/j.yhbeh.2009.03.005>
PMID:19306881
48. Love T, Smith YR, Persad CC, Tkaczyk A, Zubieta JK. Short-term hormone treatment modulates emotion response circuitry in postmenopausal women. *Fertil Steril*. 2010; 93:1929–37.
<https://doi.org/10.1016/j.fertnstert.2008.12.056>
PMID:19243753
49. Fama R, Sullivan EV. Thalamic structures and associated cognitive functions: Relations with age and aging. *Neurosci Biobehav Rev*. 2015; 54:29–37.
<https://doi.org/10.1016/j.neubiorev.2015.03.008>
PMID:25862940
50. Guedj C, Vuilleumier P. Functional connectivity fingerprints of the human pulvinar: Decoding its role in cognition. *Neuroimage*. 2020; 221:117162.
<https://doi.org/10.1016/j.neuroimage.2020.117162>
PMID:32659353
51. Ivanov I, Bansal R, Hao X, Zhu H, Kellendonk C, Miller L, Sanchez-Pena J, Miller AM, Chakravarty MM, Klahr K, Durkin K, Greenhill LL, Peterson BS. Morphological abnormalities of the thalamus in youths with attention deficit hyperactivity disorder. *Am J Psychiatry*. 2010; 167:397–408.
<https://doi.org/10.1176/appi.ajp.2009.09030398>
PMID:20123910